Iranian Society of Acoustics and Vibration
The 15th ISAV2025 International Conference on Acoustics and Vibration
24-25 Dec 2025 Tehran- Iran

Composition-Tuned Acoustic Damping in He–Ar Mixtures via Carbon Nanotube Absorption: A Molecular Dynamics Study

Fahimeh Mokhtari [a], Mohammad Kamalvand [a*], Mohammad Mehdi Jalili [b]

[a] *Department of Chemistry, Faculty of Science, Yazd University, Yazd, Iran.*

[b] *Department of Chemistry, Faculty of Science, Yazd University, Yazd, Iran.*

** Mohammad Kamalvand e-mail: kamalvand@yazd.ac.ir*

Abstract

Noise pollution is a critical environmental concern, driving the need for compact nanoscale acoustic absorbers. Carbon nanotubes (CNTs) are promising candidates due to their high stiffness, tunable geometry, and strong gas-solid coupling. This study employs molecular dynamics (MD) simulations to investigate longitudinal wave propagation and attenuation in helium-argon mixtures (He mole fraction: 0.0 to 1.0), both with and without a single-walled CNT absorber. The results show that sound velocity increases monotonically with helium fraction, consistent with the reduction in mean molar mass. In contrast, the attenuation coefficient exhibits a non-monotonic dependence, peaking near the equimolar mixture due to enhanced Ar–He collision rates. The presence of the CNT modifies attenuation in a composition-dependent manner: at low helium fractions (≤ 0.5), total attenuation is suppressed because of standing-wave nodes and strong gas-phase damping, while at high helium fractions (≥ 0.7), attenuation is amplified as energetic helium atoms efficiently transfer momentum to the CNT. These findings clarify the microscopic mechanisms of nanoscale acoustic absorption and provide valuable MD benchmarks for the rational design of next-generation acoustic devices.

Keywords: Acoustic attenuation; Helium–argon mixtures; Standing waves; Gas–nanostructure interactions.

1. Introduction

Noise pollution is a growing environmental and public-health concern, linked to hearing loss, cardiovascular disease, sleep disruption, and psychological stress [1–2]. Traditional porous and fibrous absorbers are commonly used, but their effectiveness is often limited in bandwidth and adaptability [3, 4]. This has driven interest in compact nanoscale acoustic absorbers capable of broadband attenuation.

Nanoscale absorbers, with high surface-to-volume ratios and tunable structures, offer enhanced mechanical properties and energy dissipation [5, 6]. Among them, carbon nanotubes (CNTs) are par-

ticularly promising due to their high stiffness, chemical stability, and ability to confine gas within their hollow cores, enabling strong gas–structure interactions [7–9]. Experimental studies have shown that incorporating CNTs into porous hosts improves macroscopic acoustic absorption, especially at low frequencies, with taller and less dense CNT forests further enhancing performance [10, 11].

Molecular dynamics (MD) simulations provide unique insights into the microscopic mechanisms of acoustic propagation and dissipation. They allow direct calculation of wave fields, energy transfer, and damping at fluid–solid interfaces [8, 10, 12]. Previous studies have demonstrated that CNTs can couple with propagating acoustic waves, excite additional vibrational modes, and enhance energy dissipation. Computational and Monte Carlo methods have also clarified gas adsorption and transport inside CNTs, revealing strong dependence on gas type and nanotube geometry [13, 14].

Helium–argon mixtures have been extensively studied for applications in thermo-acoustic engines, plasma physics, and shock-wave dynamics due to their contrasting acoustic properties [15, 16]. Experimental and theoretical works have provided benchmarks for sound absorption, revealed phenomena such as “fast sound” in dense mixtures, and characterized sound velocity across broad pressure and temperature ranges [17–19]. Despite this, the combined influence of CNT absorbers and He–Ar mixtures on acoustic attenuation remains unexplored at the molecular scale.

In this study, we employ MD simulations to systematically investigate longitudinal acoustic wave propagation and attenuation in He–Ar mixtures with varying helium fractions (0–1), both with and without a CNT absorber fixed near a reflective boundary. Acoustic parameters—including sound speed, wavenumber, and attenuation—are extracted from standing-wave velocity profiles using nonlinear fitting. This work clarifies how gas composition and nanoscale absorbers interact, identifies conditions where CNTs enhance or reduce attenuation, and provides molecular-scale benchmarks for the design of next-generation acoustic devices.

2. Theoretical and Molecular Dynamics Framework

2.1 Standing Wave Theory

Longitudinal acoustic waves propagate through alternating compressions and rarefactions of the gas, with negligible net pressure fluctuations [14]. Early molecular simulations confirmed such nanoscale acoustic behavior in monatomic gases, validating molecular-level wave propagation [14]. Subsequent studies extended this framework to more complex fluids and confined systems, showing how oscillating boundaries generate acoustic excitations and how attenuation can be quantified from velocity fields [20].

In MD simulations, standing waves are typically generated by imposing oscillatory motion on one wall and a reflective boundary at the opposite end. The wall displacement $Z(t)$ and velocity $V(t)$ are defined as:

$$Z_\omega(t) = a(1 - \cos\omega t) \tag{1}$$

$$V_\omega(t) = a\omega \sin\omega t \tag{2}$$

Where a is the oscillation amplitude and ω the angular frequency. These oscillations generate plane acoustic waves along the propagation axis:

$$v_i(z,t) = v_0 \exp[i(\omega t - kz) - mz] \tag{3}$$

Where k is the wavenumber and m is the attenuation coefficient. Reflection at the fixed boundary produces

$$v_r(z,t) = -v_0 \exp[i(\omega t - k(2l_z - z)) - m(2l_z - z)] \tag{4}$$

Where l_z is the domain length. The superposition yields a standing wave expressed as:

$$v(z,t) = A(z)\sin wt + B(z)\cos wt \tag{5}$$

Amplitudes $A(z)$ and $B(z)$ are extracted via nonlinear fitting to the simulation velocity data [12], allowing robust estimation of k and m. A custom MATLAB routine minimizes the combined squared errors across both equations, improving reliability over standard tools sensitive to initial guesses.

2.2 Molecular Dynamics Simulation Setup

The simulation domain is a rectangular box containing He–Ar mixtures with mole fractions x-He = 0.0, 0.1, 0.3, 0.5, 0.7, 0.9, 1.0 , with and without a single-walled CNT (length 25 nm, diameter 2.98 nm) near the reflective boundary (Fig. 1). All simulations were performed at 1.5 GHz. The lateral box dimensions were fixed at 150 Å, while the longitudinal length along the propagation axis was set to approximately half the acoustic wavelength for each composition.

The oscillating wall at *z=0* generates the wave using a rigid, structureless boundary that transfers momentum without absorbing energy. The opposite wall is fully reflective, producing standing waves. Argon and helium are selected for their complementary acoustic properties. Ar provides a reliable reference, while He, with lower molar mass and higher sound speed, allows assessment of composition-dependent effects. Both are monatomic, eliminating internal vibrational complications.

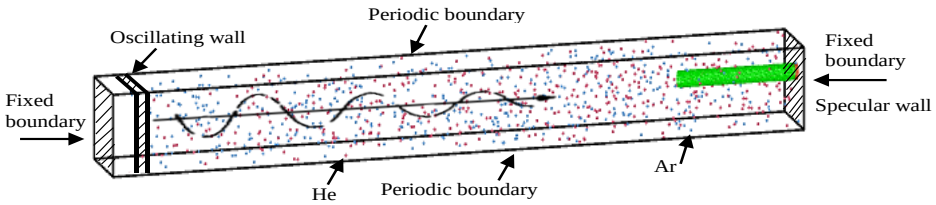

Figure 1. Schematic of the MD simulation setup showing the oscillating wall, reflective boundary, CNT absorber, and Ar–He gas mixture.

2.2.1 Interaction Potentials

Covalent bonding within the CNT was described using the three-body Tersoff potential [21], accurately capturing sp^2 carbon dynamics. Non-bonded gas–gas and gas–CNT interactions were modeled via the Lennard–Jones (12–6) potential, with mixed interactions obtained through Lorentz–Berthelot combining rules. Gas–wall interactions employed Lennard–Jones potentials, with (9–3) for the oscillating wall and (12–6) for the reflective wall, using parameters consistent with the pure gas [22]. The relevant Lennard–Jones parameters are summarized in Table 1.

Table 1. Lennard–Jones parameters used for gas–gas and gas–CNT interactions.

Interaction	σ (nm)	ε (kcal/mol)	Reference
Ar–Ar	0.340	0.238	[8]
Ar–C	0.338	0.115	[8]
He–He	0.256	0.0204	[7]
He–C	0.298	0.0337	[7]
Ar–He	0.298	0.0697	[22]
$\sigma_{i\text{-}j} = (\sigma_{i\text{-}i} + \sigma_{j\text{-}j})/2$		$\varepsilon_{i\text{-}j} = \sqrt{(\varepsilon_{i\text{-}i} \times \varepsilon_{j\text{-}j})}$	

2.2.2 Simulation Protocol

All MD simulations were performed using LAMMPS [23]. The gas was maintained at 273 K and 1 atm, with density adjusted for each Ar–He composition. Acoustic waves were generated by harmonically oscillating a structureless wall at 1.5 GHz with a velocity amplitude of 49.69 m/s, modeled via a Lennard–Jones (9–3) potential. Such a high excitation frequency is commonly used in MD because audible-range waves (kHz) cannot be simulated within nanosecond timescales. Since the wall contains no atoms, all dissipation arises from the gas and CNT. The opposite wall was fully reflective, using a Lennard–Jones (12–6) potential.

Initial gas velocities followed a Gaussian distribution. Systems were equilibrated for 10 ns with a 0.5 fs timestep under a Langevin thermostat applied to gas and mobile CNT atoms. Acoustic propagation was then simulated for 100 oscillation periods with a 1 fs timestep, maintaining thermostats to control temperature.

3. Results and Physical Insights

3.1 Acoustic properties of Ar–He mixtures (gas phase)

Table 2 reports the sound velocity, wavenumber, and attenuation coefficient obtained from nonlinear fitting of the standing-wave velocity components for all Ar–He compositions at f= 1.5 GHz.

Table 2. Extracted acoustic parameters from MD simulations for different Ar–He mole fractions at f=1.5 GHz (number of atoms (N), simulation box length (L_Z), wave number (k), sound velocity (c), and attenuation coefficient (m)).

Gas	L_Z[nm]	N	$m \times 10^7\,[\mathrm{m}^{-1}]$	$k \times 10^7\,[m^{-1}]$	$c[\mathrm{m.s}^{-1}]$
$x_{He} = 0.0$	150	978	0.8206	0.0231	407.10
$x_{He} = 0.1$	150	969	0.9701	0.0220	427.86
$x_{He} = 0.3$	150	969	1.0613	0.0189	499.36
$x_{He} = 0.5$	150	970	1.1788	0.0143	658.97
$x_{He} = 0.7$	200	1292	0.8164	0.0109	866.14
$x_{He} = 0.9$	250	1615	0.3318	0.0078	1229.10
$x_{He} = 1.0$	365	2359	0.2981	0.0071	1331.00

The results show that the sound speed increases monotonically with helium mole fraction, consistent with the ideal-gas relation (Eq. 6), confirming the correctness of the MD setup.

$$c \approx \sqrt{\gamma \frac{RT}{M_{mix}}} \tag{6}$$

Where γ is the heat capacity ratio, R is the gas constant, T is the temperature, and M_{mix} is the mean molar mass of the mixture. Since helium has a significantly lower molar mass than argon, increasing its mole fraction reduces M and thereby enhances the sound velocity.

In contrast, the attenuation coefficient exhibits non-monotonic behaviour, it rises with helium addition, peaks near the equimolar mixture, and decreases at higher helium fractions. This arises from a combination of continuum viscous–thermal losses and diffusive dissipation due to interspecies collisions [26-28]:

$$m_{tot} \approx m_{viscothermal} + m_{\text{diffusive}} \tag{7}$$

At low He fractions, the number of Ar–He collisions increases rapidly, enhancing dissipation. Near equimolar composition, the maximum disparity in molecular velocities produces peak attenuation. At high He fractions, the viscous–thermal contribution drops sharply, and reduced Ar–He collisions along with higher He diffusivity lower the overall attenuation. Additional kinetic effects in He-rich mixtures (longer mean free paths, higher Knudsen number) further reduce dissipation.

Overall, this analysis establishes two key points: Sound speed increases monotonically with helium content and Attenuation is composition-dependent, peaking at intermediate He fractions due to competing viscous-thermal and diffusive mechanisms.

These baseline results provide a reference for evaluating how the CNT absorber affects energy dissipation in the subsequent section.

3.2 Acoustic propagation in Ar–He mixtures with a CNT absorber

Fig. 2 presents a comparison between the standing-wave velocity profiles in the pure gas phase and in the presence of the CNT absorber for all Ar–He compositions. The introduction of the CNT does not modify the trend of sound speed, confirming that the nanotube primarily affects dissipative mechanisms rather than the fundamental wave propagation characteristics. However, a clear composition dependent modification of the velocity amplitudes is observed.

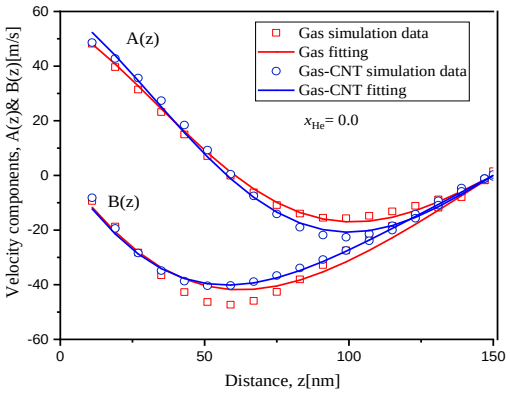

(a)

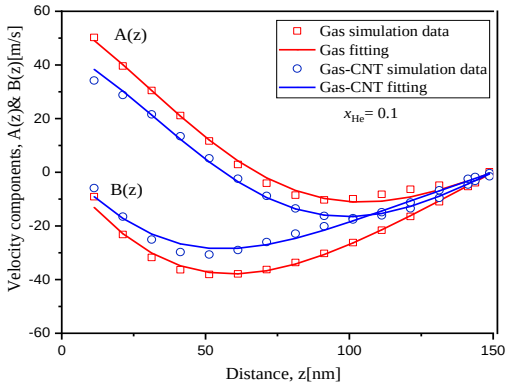

(b)

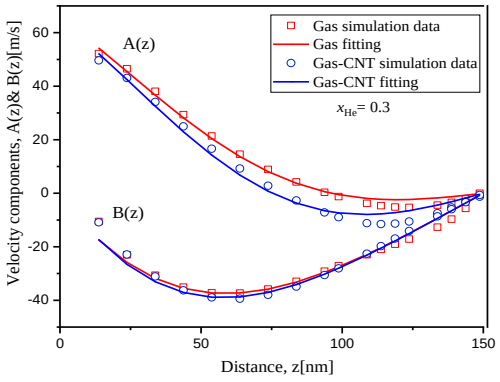

(c)

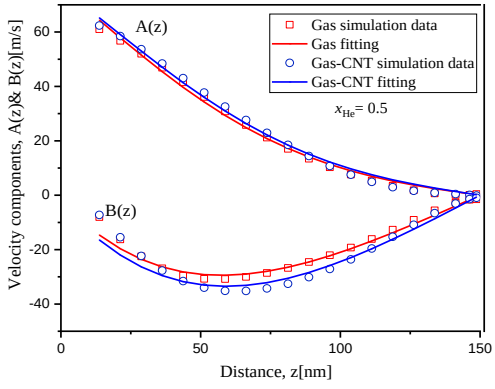

(d)

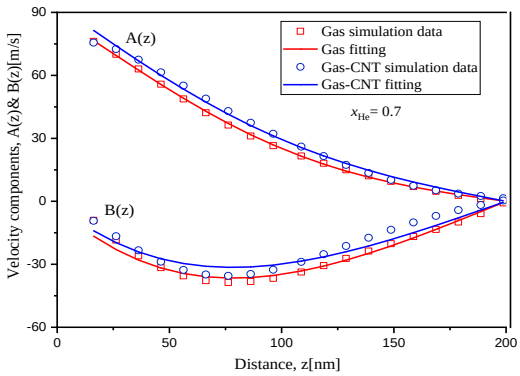

(e)

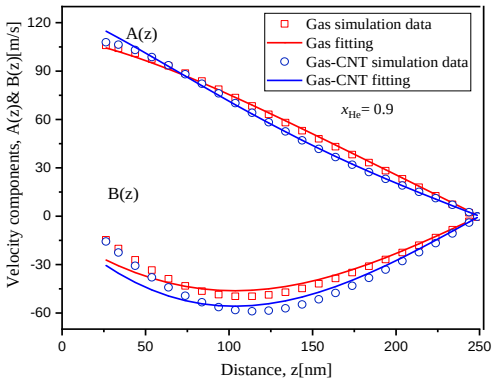

(f)

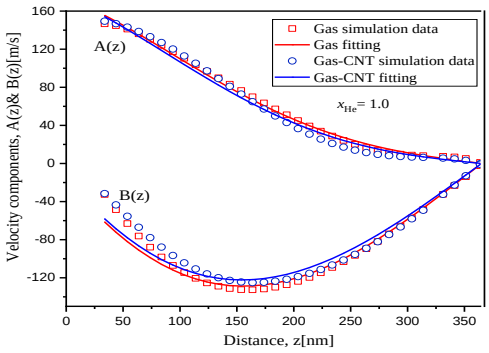

(g)

Figure 2. Fitted velocity profiles for acoustic wave propagation in Ar–He mixtures at different helium mole fractions in the presence of CNT.

For argon-rich mixtures (x_He ≤ 0.5), the standing-wave amplitudes are noticeably reduced. This behavior reflects the stronger collisional damping in heavier-gas environments, where the higher mass and lower thermal velocity of argon lead to more effective momentum-diffusion during wave compression and rarefaction. As the helium content increases toward x_He ≈ 0.5, the amplitudes gradually increase. This intermediate regime is characterized by a balance between reduced viscous–thermal damping and enhanced Ar–He collision rates, which together allow larger velocity oscillations to develop within the standing-wave field. At higher helium fractions (x_He ≥ 0.7), the velocity amplitudes continue to rise due to the dominance of the lighter and faster species. The reduced intrinsic damping of He-rich mixtures permits more acoustic energy to propagate across the domain, resulting in a stronger local velocity field at the CNT location. This trend directly influences the amount of energy available for nanotube excitation.

Quantitative acoustic parameters extracted from nonlinear fitting are reported in Table 3. The attenuation coefficients exhibit the same non-monotonic composition dependence observed in the gas-only systems: attenuation increases with added helium, peaks near the equimolar composition, and diminishes again in He-rich limits. The consistently high goodness-of-fit ($R^2 > 0.96$) confirms the robustness of the fitting procedure.

An interesting deviation from the general trend occurs at x_He = 0.1, where the CNT unexpectedly reduces the total attenuation relative to pure Ar. As illustrated in Fig. 2(b), a velocity node forms upstream of the CNT (approximately 112–125 nm), significantly decreasing the local kinetic-energy flux available for absorption. As a result, the nanotube operates in an energy-deficient region of the standing-wave field and contributes minimally—or even negatively—to overall dissipation. This observation demonstrates that CNT absorption efficiency is strongly influenced not only by

gas composition and intrinsic damping, but also by the relative placement of the absorber with respect to the nodal–antinodal structure of the wave.

Table 3. Acoustic parameters from MD simulations and corresponding statistical fitting results for Ar–He mixtures with a CNT absorber at different helium mole fractions.

Gas+ CNT	N	$m \times 10^7 [\mathrm{m}^{-1}]$	$k \times 10^7 [m^{-1}]$	$c[\mathrm{m.s}^{-1}]$	RMSE	R^2
$x_{He} = 0.0$	8976	0.978	0.0238	396.22	1.431	0.993
$x_{He} = 0.1$	9945	0.925	0.0248	379.52	1.316	0.989
$x_{He} = 0.3$	9945	1.046	0.0209	450.65	1.992	0.985
$x_{He} = 0.5$	9946	1.071	0.0149	631.49	2.165	0.982
$x_{He} = 0.7$	10268	0.854	0.0095	987.16	2.522	0.981
$x_{He} = 0.9$	10591	0.465	0.0080	1174.00	3.825	0.980
$x_{He} = 1.0$	11335	0.317	0.0071	1331.30	7.870	0.968

Taken together, these findings reveal that CNT-based nanoscale acoustic absorption is not a uniform additive effect but emerges from the combined influence of (i) gas-phase damping, (ii) molecular velocities, (iii) interspecies collision dynamics, and (iv) the spatial structure of the standing wave. Consequently, understanding and controlling absorber placement and gas composition are essential for optimizing nanoscale acoustic dissipation.

4. Conclusion

Molecular dynamics simulations were performed to quantify how gas composition and nanoscale absorption jointly shape acoustic wave propagation in He–Ar mixtures. The results show that the sound speed increases monotonically with helium fraction, consistent with the reduction in mean molar mass. In contrast, the attenuation coefficient exhibits a distinctly non-monotonic behavior: it rises in Ar-rich mixtures, reaches a maximum near the equimolar composition, and decreases again as the mixture becomes He-dominated. This peak originates from enhanced Ar–He interspecies collision rates, which intensify diffusive and viscous–thermal dissipation.

Incorporating a single CNT absorber revealed that its influence is strongly composition-dependent. Rather than imposing a uniform additional loss, the CNT modifies wave dissipation according to the interplay between gas-phase damping, molecular velocities, and the spatial energy distribution of the standing wave. In He-rich mixtures, where intrinsic gas damping is weak, more acoustic energy reaches the nanotube and CNT-mediated dissipation increases. Conversely, in Ar-rich conditions or when the CNT coincides with a velocity node the absorber receives little energy and may even reduce net attenuation.

Overall, the findings demonstrate that nanoscale acoustic absorption cannot be understood solely from material properties of the absorber. Instead, it emerges from the coupled effects of gas composition, molecular collision dynamics, and wave-field geometry. These insights provide molecular-level benchmarks for optimizing CNT-based acoustic absorbers and offer a predictive foundation for future experimental validation and multiscale modeling of acoustic dissipation in gas–nanostructure systems.

REFERENCES

1. J. Nan, L. Yu, M. Du, J. Meng, Z. Dong, M. Miao, et al., "Highly efficient underwater acoustic absorber designed by filled-microperforated plate-like structure: Aging and life prediction", Polymer Testing, (2023).
2. D. Yin, Y. Liu, Y. Wang, Y. Gao, S. Hu, L. Liu, et al., "Finite element solution for dynamic mechanical parameter influence on underwater sound absorption of polyurethane-based composite", International Journal of Molecular Sciences, (2022).
3. N. Rastegar, A. Ershad-Langroudi, H. Parsimehr, G. Moradi, "Sound-absorbing porous materials: a review on polyurethane-based foams", Iranian Polymer Journal, (2022).
4. L. Cao, Q. Fu, Y. Si, B. Ding, J. Yu, "Porous materials for sound absorption", Composites Communications, (2018).
5. A. Hosseinpour, A. A. Katbab, A. Ohadi, "Improving the sound absorption of a highly deformable nanocomposite foam based on ethylene-propylene-diene-monomer (EPDM) infused with multi-walled carbon nanotubes (MWCNTs) to absorb low-frequency waves", European Polymer Journal, (2022).
6. M. Ahmadi, M. Talebitooti, R. Talebitooti, "Analytical investigation on sound transmission loss of functionally graded nanocomposite cylindrical shells reinforced by carbon nanotubes", Mechanics Based Design of Structures and Machines, (2022).
7. Z. Bolboli Nojini, A. Abbas Rafati, S. Majid Hashemianzadeh, S. Samiee, "Predicting helium and neon adsorption and separation on carbon nanotubes by Monte Carlo simulation", Journal of Molecular Modeling, (2011).
8. M. Ayub, A. Zander, D. Huang, C. Howard, B. Cazzolato, "Molecular dynamics simulations of acoustic absorption by a carbon nanotube", Physics of Fluids, (2018).
9. M. Kohestanian, Z. Sohbatzadeh, S. Rezaee, "Mechanical properties of continuous fiber composites of cubic silicon carbide (3C-SiC)/different types of carbon nanotubes (SWCNTs, RSWCNTs, and MWCNTs): A molecular dynamics simulation", Materials Today Communications, (2020).
10. J. Xiong, J. Liu, W. Lin, Y. Li, L. Liao, M. Wen, et al., "Enhanced Broadband Acoustic Absorption in Commercial Foam via Multiwall Carbon Nanotube-Induced Pore Reconstruction", Advanced Science, (2025).
11. M. Ayub, A. C. Zander, C. Q. Howard, B. S. Cazzolato, "Acoustic absorption behaviour of carbon nanotube arrays", INTER-NOISE 2014, (2014).
12. M. Ayub, A. C. Zander, C. Q. Howard, D. M. Huang, B. S. Cazzolato, "Molecular dynamics simulations of sound wave propagation in a gas and thermo-acoustic effects on a carbon nanotube", Journal of Computational Acoustics, (2015).
13. D. A. Damasceno, H. M. Cezar, T. D. Lanna, A. Kirch, C. R. Miranda, "Mechanical and adsorption properties of greenhouse gases filled carbon nanotubes", arXiv preprint arXiv:230711708, (2023).
14. N. G. Hadjiconstantinou, A. L. Garcia, "Molecular simulations of sound wave propagation in simple gases", Physics of Fluids, (2001).
15. I. Kandemir, F. E. Sevilgen, "Molecular dynamics simulation of helium–argon gas mixture under various wall conditions", Molecular Simulation, (2008).
16. F. Sharipov, V. J. Benites, "Transport coefficients of helium-argon mixture based on ab initio potential", The Journal of Chemical Physics, (2015).
17. A. Law, N. Koronaios, R. B. Lindsay, R. Stavseth, "Sound Attenuation in Helium-Argon Mixtures", The Journal of the Acoustical Society of America, (1965).
18. C. Wedler, J. M. Trusler, "Speed of Sound Measurements in Helium at Pressures from 15 to 100 MPa and Temperatures from 273 to 373 K", Journal of Chemical & Engineering Data, (2023).
19. A. T. Azizi, "Study of Xenon, Argon, Neon and Helium Absorption on Carbon Nanotube Bundles with various Diameters using molecular dynamics simulation", Research Review International Journal of Multidisciplinary, (2021).
20. Y. Asano, H. Watanabe, H. Noguchi, "Molecular dynamics simulation of soundwave propagation in a simple fluid", The Journal of Chemical Physics, (2020).
21. J. Tersoff, "New empirical approach for the structure and energy of covalent systems", Physical Review B, (1988).
22. M. P. Allen, D. J. Tildesley, Computer Simulation of Liquids, Oxford University Press, (2017).
23. S. Plimpton, "Fast parallel algorithms for short-range molecular dynamics", Journal of Computational Physics, (1995).
24. P. W. Atkins, J. De Paula, J. Keeler, Atkins' Physical Chemistry, Oxford University Press, (2023).
25. L. E. Kinsler, A. R. Frey, A. B. Coppens, J. V. Sanders, Fundamentals of Acoustics, John Wiley & Sons, (2000).
26. A. D. Pierce, Acoustics: An Introduction to Its Physical Principles and Applications, Springer, (2019).
27. K. F. Herzfeld, T. A. Litovitz, Absorption and Dispersion of Ultrasonic Waves, Academic Press, (2013).
28. F. A. Angona, "The absorption of sound in gas mixtures", The Journal of the Acoustical Society of America, (1953).